Supporting Information

One-Dimensional Organic Metal Halide Nanoribbons with Dual Emission

Sujin Lee,[a] Rijan Karkee,[b] Azza Ben-Akacha,[a] Derek Luong,[c] J.S. Raaj Vellore Winfred,[a] Xinsong Lin,[a] David A. Strubbe,[*b] and Biwu Ma[*a]

[a] Department of Chemistry and Biochemistry, Florida State University, Tallahassee, Florida 32306, United States

[b] Department of Physics, University of California, Merced, Merced, CA 95343, United States

[c] Department of Biology Science, Florida State University, Tallahassee, Florida 32306, United States

Materials and Characterization

Materials. Lead chloride ($PbCl_2$, 99.99 %), tetraethylenepentamine pentahydrochloride (98%), HCl (37%) were purchased from Sigma Aldrich and were used without further purification.

Synthesis of $C_8H_{28}N_5Pb_3Cl_{11}$. Lead chloride (0.11 g, 0.40 mmol) and tetraethylenepentamine pentahydrochloride (0.05 g, 0.13 mmol) were added to a vial with 5 mL of HCl and 5 mL of water. The mixture was stirred and heated at 100 ^oC for 1 hour. Then the solution was left to cool slowly to room temperature. Colorless thin platelike crystals were obtained with the size of around 2~3 mm. The crystals were washed with water and acetone and dried under reduced pressure. The yield was calculated at ~ 67 %. Elemental analysis was performed by Atlantic Microlabs, Atlanta, GA. $C_8H_{28}N_5Pb_3Cl_{11}$: Anal, Calc. C, 7.97; H, 2.34; N, 5.81; Cl, 32.34 Found: C, 7.96; H, 2.33; N, 5.61; Cl, 32.07.

Single crystal X-ray crystallography: The single crystal structure was solved using Rigaku XtaLAB Synergy-S diffractometer equipped with a HyPix-6000HE Hybrid Photon Counting (HPC) detector and Cu microfocus sealed X-ray sources. The crystal was mounted in cryoloop

with Paratone-N oil. The data were collected at 150.00(10) K. The structures were solved using Olex2 software where XT[1] structure solution program using Intrinsic Phasing and the XL[2] refinement package using Least Squares minimization were employed in solving and refining the structures, respectively. Table S1 summarizes the refinement details and the resulting factors. A CIF has been deposited with the CCDC (2244486). VESTA was used as the crystal structure visualization software for the images presented in the manuscript.

Powder X-ray Diffraction: The PXRD analysis was performed on Rigaku MiniFlex powder X-Ray diffractometer with a copper anode-type generator (Cu-Ka, λ =0.154 nm, 40 kV, 15 mA) and D/teX Ultra detector. The diffraction pattern was scanned over the angular range of 5-50^{o} (2θ) with a step size of 0.05 at room temperature. Simulated powder patterns were calculated in the Mercury software from the corresponding crystallographic information file from SCXRD experiment.

Thermogravimetry Analysis: TGA was conducted on a TA Instruments TGA 550 system. The sample was heated from room temperature to 250 ^{o}C at a rate of 5 ^{o}C·min^{-1}, then heated at a rate of 10 ^{o}C·min^{-1} to 800 ^{o}C under an argon flux of 40 mL·min^{-1}.

Photoluminescence Steady-State Studies: Steady-state PL spectra of $C_8H_{28}N_5Pb_3Cl_{11}$ were measured at room temperature and at 77 K (liquid nitrogen was used to cool the sample) on a FS5 spectrofluorometer (Edinburgh Instruments).

Absorption Spectrum Measurements: Absorption spectra of $C_8H_{28}N_5Pb_3Cl_{11}$ were obtained at room temperature through a synchronous scan in an integrating sphere incorporated into the spectrofluorometer (FS5, Edinburgh Instruments).

Time-resolved photoluminescence: The lifetimes in the range of nanosecond were measured at room temperature using time-correlated single photon counting on a FS5 spectrofluorometer (Edinburgh Instruments) with data collection for 10000 counts. The samples were excited by an

Edinburgh EPL-365 picosecond pulsed diode laser and the emission counts was monitored at corresponding emission maximums. The long lifetime in the range of microsecond was measured using the Edinburgh Instruments LP980-KS laser flash photolysis spectrometer using an Nd:YAG pump laser as the excitation source. The emission counts were monitored at the corresponding emission maximum, and the data was obtained to 10000 counts. The intensity average lifetime is defined as $\langle\tau\rangle = \Sigma\, a_i\tau_i^2/\Sigma\, a_i\tau_i$, where τ_i represents the decay time, and α_i represents the amplitude of each component.

Photoluminescence Intensity Dependence on Excitation Power Density: The power-dependent PL intensity measurement was performed on an Edinburgh Instruments LP980-KS transient absorption spectrometer using a Continuum Nd:YAG laser (Surelite EX) pumping a Continuum optical parametric oscillator (Horizon II OPO) to provide 360 nm 5 ns pulses at 1 Hz. The pump beam profile was carefully defined using collimated laser pulses passed through an iris set to an area of 0.38 cm^2. The pulse intensity was monitored by a power meter (Ophir PE10BF-C), detecting the reflection from a beam splitter. Detection consisted of an Andor Intensified CCD (1024 × 256 element) camera, collecting a spectrum from 287 to 868 nm and gated to optimize PL collection (typically a 30−50 ns gate depending on the PL lifetime, starting immediately following the 5 ns laser pulse). Twenty collections were averaged at each power level with every laser pulse monitored to determine the average intensity. The PL was determined at the maximum of the PL emission curve.

Photoluminescence Quantum Efficiencies: The PLQE was obtained using a Hamamatsu Quantaurus-QY Spectrometer (model C11347-11) equipped with a xenon lamp, integrated sphere sample chamber, and CCD detector. The PLQE was calculated by using the equation: $\eta_{QE} = I_S/(E_R - E_S)$, in which I_S represents the luminescence emission spectrum of the sample, E_R is the spectrum

of the excitation light from the empty integrated sphere (without the sample), and E_S is the excitation spectrum for exciting the sample.

Computational Methods: Calculations used Quantum ESPRESSO version 6.4.1[3] and Perdew-Burke-Ernzerhof (PBE)[4] functional. While dispersion is physically present in this material, we find that the interactions defining the structure are well described by PBE, whereas adding the Grimme D2 dispersion correction[5] gave lattice parameters with too small b (a = 11.28 Å, b = 14.28 Å, c = 31.92 Å, $\alpha = \beta = \gamma = 90°$). The electronic properties for a given structure are unaffected by the use of a dispersion correction. ONCV pseudopotentials[6] from PseudoDojo[7] were used. A wavefunction energy cutoff of 816 eV was used, and a 3×2×1 half-shifted *k*-grid for self-consistent field (SCF) calculations. Forces and stresses were relaxed below 10^{-4} Ry/bohr and 0.1 kbar, respectively. Density of states calculations used a 9×6×3 half-shifted *k*-grid and a broadening of 0.05 eV. Optical absorption spectra computed with the random phase approximation (RPA) in BerkeleyGW code,[8] used 100 occupied states and 150 unoccupied states, 10×2×2 k-point sampling, and 0.1 eV Gaussian broadening.

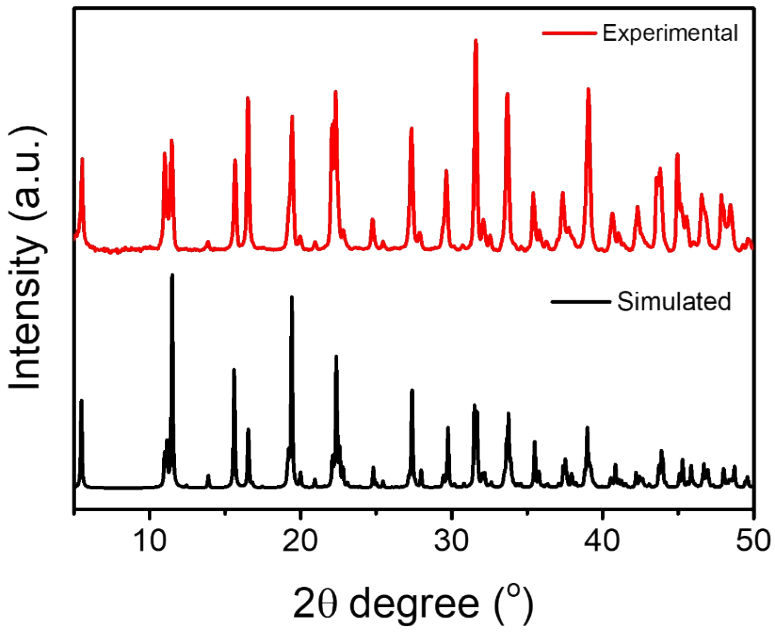

Figure S1. PXRD patterns of $C_8H_{28}N_5Pb_3Cl_{11}$ and its SCXRD simulated result.

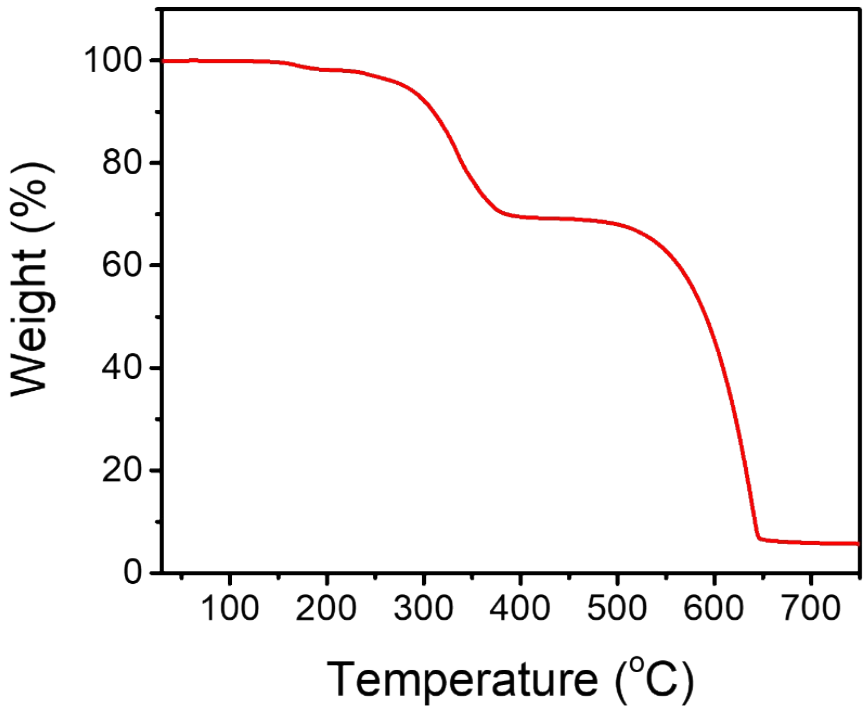

Figure S2. TGA analysis of $C_8H_{28}N_5Pb_3Cl_{11}$.

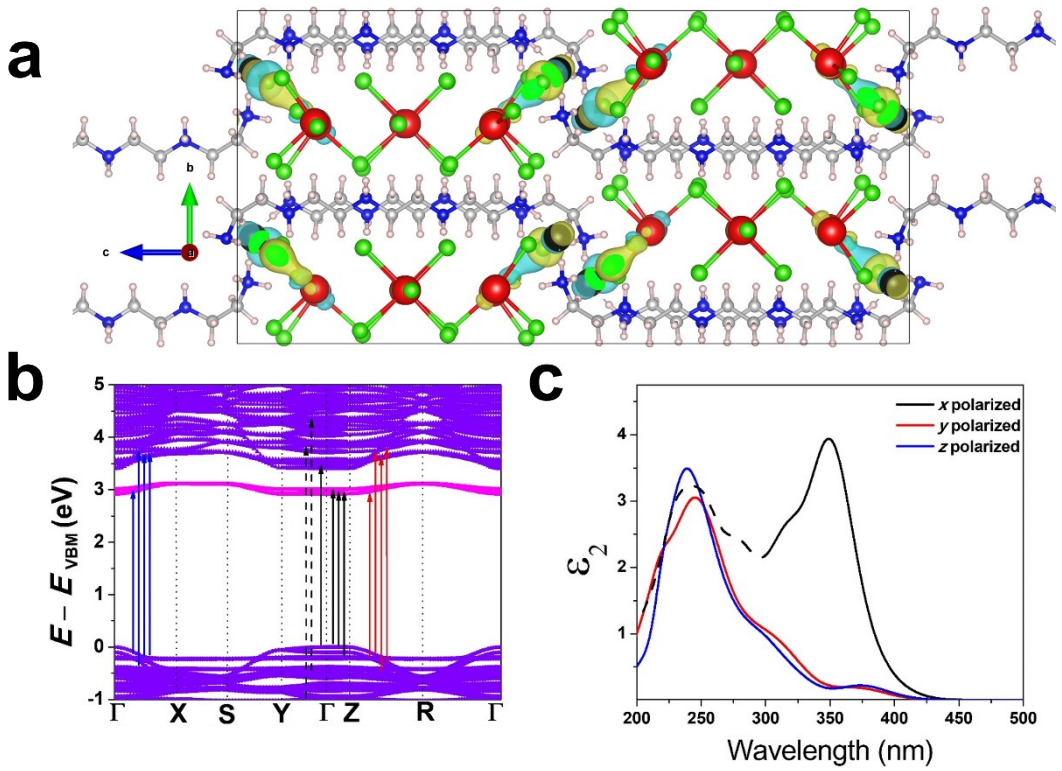

Figure S3. Calculations of structure from SCXRD containing an O atom, with formula unit $C_8H_{28}Cl_{11}N_5OPb_3$. (a) Relaxed structure with lattice parameters a = 11.32 Å, b = 15.92 Å, c = 32.15 Å, $\alpha = \beta = \gamma = 90°$; minimally different from structure without O atom. The O atom (black) makes a bond with Cl. (b) Bandstructure, showing a new flat conduction band in the gap, localized on the O-Cl bond. The next lowest conduction bands are on the Pb-Cl chain as in the structure without O, and they are pushed up slightly higher in energy. Arrows show optical transitions for peaks polarized along x (black), y (red), and z (blue) directions, where x is the direction along the Pb-Cl chains, and the solid and dotted black arrows indicate the lowest and second-lowest energy transitions. (c) Optical absorption spectrum, with x-polarized peaks are solid and dotted as in (a), showing similar features to that without O, but with somewhat modified intensities of higher peaks. Surprisingly, the transitions involved are quite different from those without O, apparently due to some small symmetry-breaking and the VBM to CBM transition becoming allowed. The O-Cl flat band makes a significant contribution despite its localization.

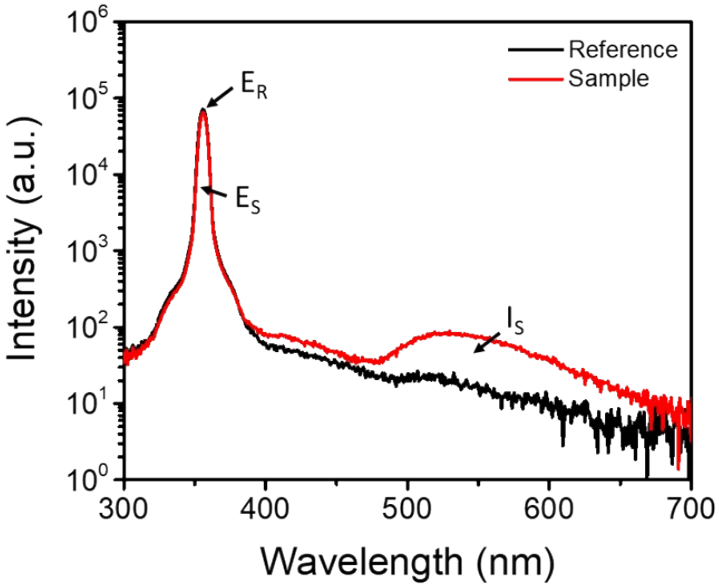

Figure S4. Excitation line of reference and emission spectrum of 1D lead chloride nanoribbons collected by an integrating sphere. The PLQE was calculated by the equation: $\eta_{QE} = I_S/(E_R - E_S)$.

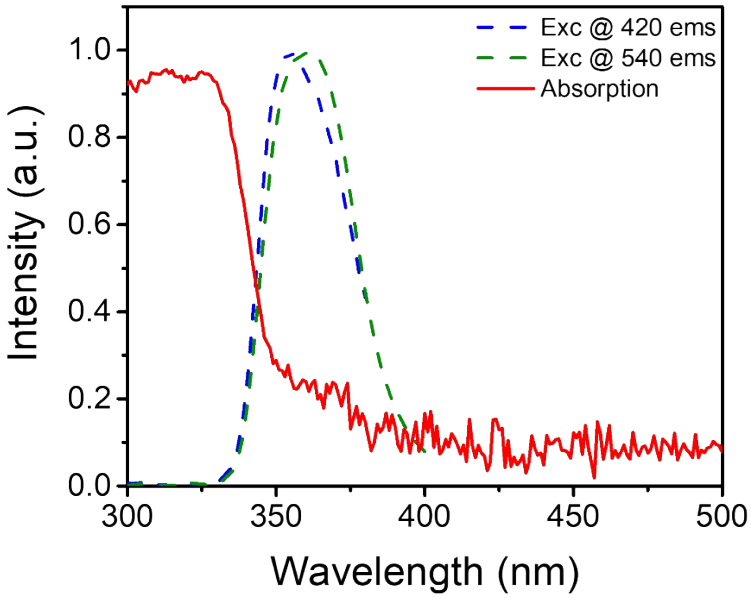

Figure S5. Absorption and excitation spectra at room temperature.

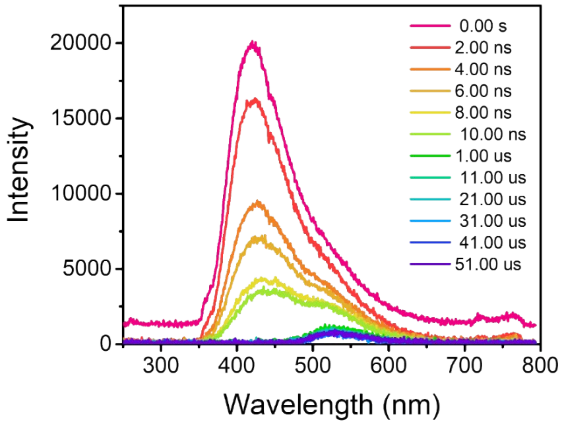

Figure S6. Emission spectra at a specific gate delay time.

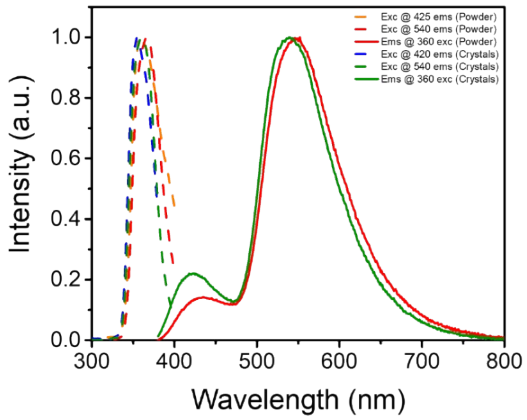

Figure S7. PL spectra of ground powder and single crystals at RT.

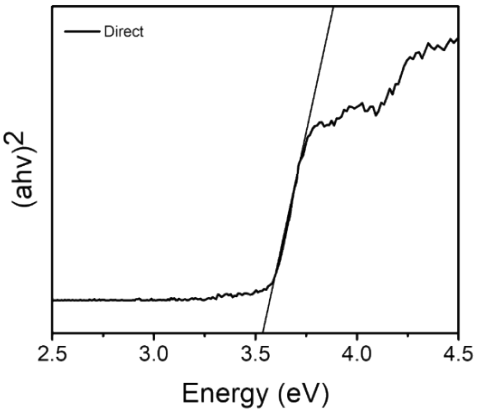

Figure S8. Tauc plot for the absorption spectrum of $C_8H_{28}N_5Pb_3Cl_{11}$ crystals.

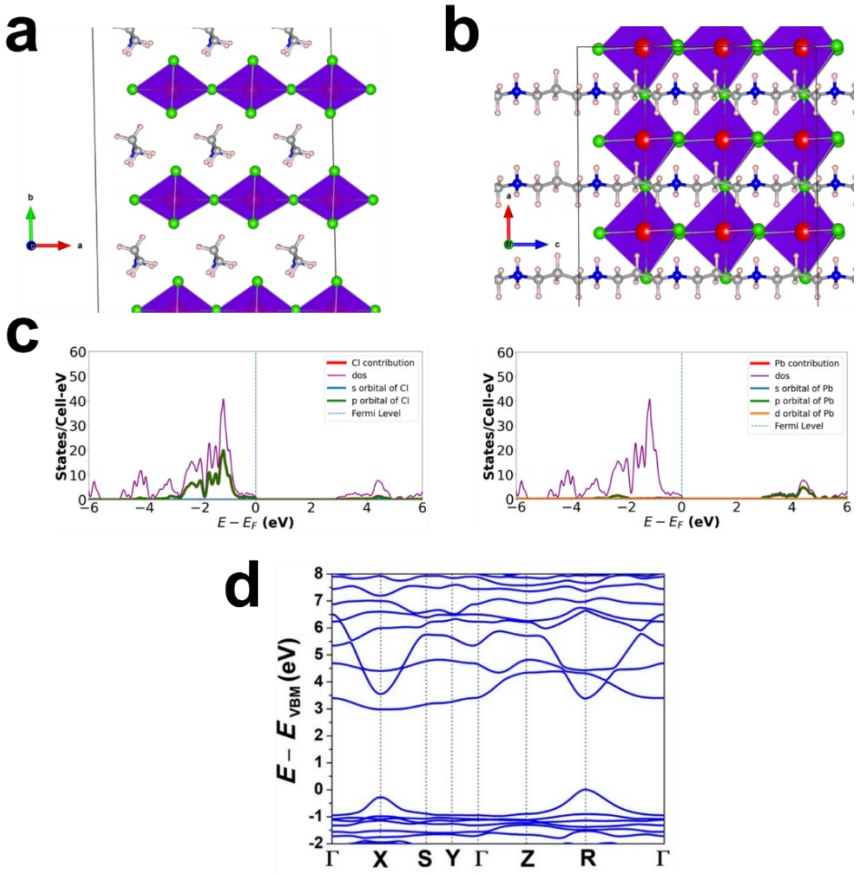

Figure S9. Calculations of hypothetical 2D sheet structure, corresponding to the 1D $C_8H_{28}N_5Pb_3Cl_{11}$, to show quantum confinement effects. The relaxed structure has lattice parameters a = 5.67Å, b = 7.92 Å, c = 4.92 Å, α = 93.35°, β = 90.33°, γ = 91.15°. The unit cell contains 16 atoms with chemical formula $C_3H_8NPbCl_3$. The Pb-Cl sheets are in the *ac* plane, separated by polymeric cations. SCF calculations used a 4×2×4 half-shifted k-grid. (a) View showing separation between layers. (b) View showing a layer. (c) Partial density of states (using a 20×2×20 half-shifted *k*-grid), showing that the VBM is primarily due to Cl *p* orbitals and CBM is primarily due to Pb *p* orbitals, as in 1D $C_8H_{28}N_5Pb_3Cl_{11}$ (Figure 4b). (d) Bandstructure, showing a smaller gap compared to the 1D structure, and an indirect gap with neither VBM nor CBM at Γ. Bands are fairly flat in the out-of-plane *y*-direction but generally dispersive in the in-plane *x*- and *z*-directions.

TABLE S1. Single crystal X-ray diffraction data for $C_8H_{30}Cl_{11}N_5OPb_3$.

Compound	$C_8H_{30}Cl_{11}N_5OPb_3$
Formula	$C_8H_{30}Cl_{11}N_5OPb_3$
Formula weight	1223.89 g/mol
Temperature	149.99(10) K
Crystal system	Orthorhombic
Space group	Pbca
a	11.36620(10) Å
b	15.87190(10) Å
c	32.1657(2) Å
α	90°
β	90°
γ	90°
V	5802.80(7) Å^3
Z	8
$\rho_{calc.}$	2.802 g/cm^3
μ	42.731 mm^{-1}
F(000)	4432.0
Crystal size	0.209 × 0.069 × 0.063 mm^3
2θ range	9.528° to 154.474°
Reflections collected	70033
Independent reflections	6022 [R_{int}=0.0434, R_{sigma}=0.0169]
Data/restraints/parameters	6022/1/259
Goodness-of-fit on F^2	1.142
Final R indexes [I>=2σ (I)]	R_1=0.0317 [a], wR_2=0.0934 [b]
Final R indexes [all data]	R_1=0.0333 [a], wR_2=0.0956 [b]

[a] $R_1 = \sum \| F_o | - | F_c \| / \sum | F_o \|$. [b] $wR_2 = [\sum w(F_o^2 - F_c^2)^2 / \sum w(F_o^2)^2]^{1/2}$.

References

1. G. M. Sheldrick, *Acta Crystallogr A Found Adv*, 2015, **71**, 3-8.
2. G. M. Sheldrick, *Acta Crystallogr A*, 2008, **64**, 112-122.
3. P. Giannozzi, O. Andreussi, T. Brumme, O. Bunau, M. Buongiorno Nardelli, M. Calandra, R. Car, C. Cavazzoni, D. Ceresoli, M. Cococcioni, N. Colonna, I. Carnimeo, A. Dal Corso, S. de Gironcoli, P. Delugas, R. A. DiStasio, Jr., A. Ferretti, A. Floris, G. Fratesi, G. Fugallo, R. Gebauer, U. Gerstmann, F. Giustino, T. Gorni, J. Jia, M. Kawamura, H. Y. Ko, A. Kokalj, E. Küçükbenli, M. Lazzeri, M. Marsili, N. Marzari, F. Mauri, N. L. Nguyen, H. V. Nguyen, A. Otero-de-la-Roza, L. Paulatto, S. Poncé, D. Rocca, R. Sabatini, B. Santra, M. Schlipf, A. P. Seitsonen, A. Smogunov, I. Timrov, T. Thonhauser, P. Umari, N. Vast, X. Wu and S. Baroni, *J Phys Condens Matter*, 2017, **29**, 465901.
4. J. P. Perdew, K. Burke and M. Ernzerhof, *Physical Review Letters*, 1996, **77**, 3865-3868.
5. S. Grimme, *Journal of Computational Chemistry*, 2006, **27**, 1787-1799.
6. M. Schlipf and F. Gygi, *Computer Physics Communications*, 2015, **196**, 36-44.
7. M. J. van Setten, M. Giantomassi, E. Bousquet, M. J. Verstraete, D. R. Hamann, X. Gonze and G. M. Rignanese, *Computer Physics Communications*, 2018, **226**, 39-54.
8. J. Deslippe, G. Samsonidze, D. A. Strubbe, M. Jain, M. L. Cohen and S. G. Louie, *Computer Physics Communications*, 2012, **183**, 1269-1289.